



Original Article

Metformin attenuates diabetes-induced osteopenia in rats is associated with down-regulation of the RAGE-JAK2-STAT1 signal axis

Rui Lin^{a,b,e,1}, Bilian Xu^{b,1}, Zhiqiang Ye^{b,1}, Yin Gao^{b,c}, Haiping Fang^b, Jintong Song^{a,b,e}, Dahong Liang^b, Lingna Liu^{b,c}, Zilong Hu^b, Min Zhang^b, Jinsong Wei^d, Feifu Deng^d, Xiangxin Zhong^d, Liao Cui^{b,**}, Yanzhi Liu^{a,b,c,e,*}

^a Zhanjiang Key Laboratory of Orthopaedic Technology and Trauma Treatment, Zhanjiang Central Hospital, Guangdong Medical University, Zhanjiang, 524037, PR China

^b Guangdong Provincial Key Laboratory for Research and Development of Natural Drug, School of Pharmacy, Guangdong Medical University, Zhanjiang, 524023, PR China

^c Marine Medical Research Institute of Zhanjiang, Zhanjiang, 524023, PR China

^d Department of Orthopedics, Affiliated Hospital of Guangdong Medical University, Zhanjiang, 524000, PR China

^e Key Laboratory of Traditional Chinese Medicine for the Prevention and Treatment of Infectious Diseases, Guangdong Provincial Administration of Traditional Chinese Medicine (Central People's Hospital of Zhanjiang), Zhanjiang, 524037, PR China

ARTICLE INFO

Keywords:

Diabetes
Bone
Osteoporosis
Osteopenia
Metformin
Fragility

ABSTRACT

Background: Osteopenia and fragile fractures are diabetes-associated complications. Many hypoglycemic drugs have effects on bone metabolism. Metformin, as a prescribed medication for type 2 diabetes mellitus (T2DM), had been reported to have osteoprotective effects beyond its hypoglycemic effect, however the potential mechanism behind these effects remains unclear. In this study, we aimed to investigate the comprehensive effects of metformin on bone metabolism in T2DM rat model and elucidate the potential mechanism.

Methods: Goto-Kakizaki spontaneous T2DM rats with significant hyperglycemia were treated with/without metformin for 20 weeks. Glucose tolerance was tested and all rats were weighed every two weeks. The osteoprotective effects of metformin in diabetic rats were determined by quantifying serum bone biomarkers, μ -CT imaging, histological staining, bone histomorphometry, and biomechanical properties analyses. Potential targets of metformin in the treatment of T2DM and osteoporosis were predicted using network pharmacology. The effects of metformin on mesenchymal stem cells (C3H10) cultured in high glucose medium were evaluated by CCK-8 assay, alkaline phosphatase (ALP) staining, qPCR and western blotting.

Results: This study demonstrated that metformin significantly attenuated osteopenia, decreased serum glucose and glycated serum protein (GSP) levels, improved bone microarchitecture, and biomechanical properties in GK rats with T2DM. Metformin significantly increased biomarkers of bone formation, and significantly decreased muscle ubiquitin C (Ubc) expression. Network pharmacology analysis found that signal transducer and activator of transcription1 (STAT1) would be a potential target of metformin for regulating bone metabolism. Metformin increased C3H10 cell viability *in vitro*, alleviated ALP inhibition caused by hyperglycemia, increased the osteogenic gene expression of runt-related transcription factor 2 (RUNX2), collagen type I alpha 1 (Col1a1), osteocalcin (OCN), and ALP, while suppressing RAGE and STAT1 expression. Metformin also increased the protein expression of Osterix and decreased that of RAGE, p-JAK2, and p-STAT1.

Conclusions: Our results demonstrate that metformin attenuated osteopenia and improved bone microarchitecture in GK rats with T2DM and significantly promoted stem cell osteogenic differentiation under high glucose condition. The effects of metformin on bone metabolism are closely associated with the suppression of RAGE-JAK2-STAT1 signaling axis.

The translational potential of this article: Our research provides experiment evidence and potential mechanistic rationale for the use of metformin as an effective candidate for diabetes-induced osteopenia treatment.

* Corresponding author. Zhanjiang Key Laboratory of Orthopaedic Technology and Trauma Treatment, Zhanjiang Central Hospital, Guangdong Medical University, Zhanjiang, 524045, PR China.

** Corresponding author.

E-mail addresses: cuiliao@163.com (L. Cui), liuyanzhi02@163.com (Y. Liu).

¹ Rui Lin, Bilian Xu, and Zhiqiang Ye contributed equally to this work and share first authorship

1. Introduction

The global prevalence of diabetes is increasing annually. The International Diabetes Federation (IDF) estimated that 536.6 million people lived with diagnosed or undiagnosed diabetes in 2021, and this will increase by 46%, to 783.2 million by 2045 [1]. T2DM accounts for >95% of all persons with diabetes [2]. Specifically, T2DM is a metabolic disease characterized by an absolute or relative deficiency of secreted insulin (INS) and decreased INS sensitivity in target organs. This is eventually followed by metabolic disorders involving fat, protein, water, and electrolytes [3]. Such metabolic disorders cause many complications, with osteoporosis and fracture being particularly significant [4–6]. Diabetes can increase the risk of fracture, and its complex pathophysiological mechanism includes hyperglycemia [7], oxidative stress [8,9] and the accumulation of advanced glycation end products (AGEs) [10,11]. These factors can deteriorate collagen properties, cause changes in bone marrow induced by obesity, release inflammatory factors and adipokines from visceral fat, and alter bone cell functions. Thus, these factors increase the risk of fracture in patients with diabetes. Risk of hip fracture is higher in older adults with T2DM than in healthy individuals [12,13]. Importantly, older adults have a higher risk of all-cause mortality during the first 3 months after hip fracture and this sustained elevated even at 5 years after fracture [14]. Evidence of restricted activities of daily living shows that ~29% of elderly persons with hip fractures do not recover to the pre-fracture level by 1-year post-fracture [15].

INS resistance promotes glucose exposure in T2DM, which in turn leads to accumulated AGEs [16]. Such accumulation in bone collagen fibers with covalent crosslinks mechanically affects the bone tissue matrix and disturbs bone remodeling, which induces bone quality degradation [17]. Patients with T2DM have increased risk of fracture due to impaired INS signaling and collagen type I glycosylation [18]. The osteogenic differentiation potential of stem cells is inhibited under high glucose concentrations [19,20]. Therefore, T2DM induces bone quality deterioration and fragility.

Metformin is the most widely prescribed medication for T2DM and the American Diabetes Association (ADA) and the European Association for the Study of Diabetes (EASD) considers it as essential medicine for T2DM patients [21]. Previous studies demonstrated that metformin can stimulate osteogenic differentiation [22,23] and inhibit the adipogenic differentiation [23] of human umbilical cord mesenchymal stem cells (hUC-MSCs). Metformin can improve the inflammatory response induced by AGEs in mouse macrophages by inhibiting the expression of the receptor for advanced glycation end products (RAGE) [24]. Furthermore, oral metformin can improve diabetic bone deterioration caused by increased RAGE expression, through alleviating the degradation of bone microstructure and stimulating the osteogenic potential of bone marrow progenitor cells (BMPCs) [25]. Therefore, previous studies suggested metformin have the effects of promoting osteogenesis and restoring bone homeostasis in addition to its hypoglycemic effects.

Here, we aimed to investigate the specific protective effects of metformin on bone in diabetic rats and also focus on the investigation of elucidating the potential mechanism behind these effects. To achieve this objective, Goto-Kakizaki (GK) rats, as an animal model of spontaneous type 2 diabetes were used for this study. GK rats were originally established by selectively inbreeding a hyperglycemic trait. INS resistance and INS secretion deficiency are the characteristics of GK rats [26].

2. Materials and methods

2.1. Animal and C3H10 cell

Eighteen 10-week-old, specific-pathogen-free male GK rats, weighing 289.34 ± 19.76 g and 16 healthy age-matched male Wistar rats weighing 258.00 ± 9.95 g (permit nos: SCXK [Shanghai] 2012–0002 for both) (Shanghai Slack Laboratory Animal Co., Ltd., Shanghai, China) were fed with standard diet and free access to water with a 12 h light–dark cycle at

$25^\circ\text{C} \pm 1^\circ\text{C}$. The C3H10 T1/2 cell line was established in 1973 from 14- to 17-day-old C3H mouse embryos [27]. These cells exhibiting fibroblast morphology in cell culture and are functionally similar to mesenchymal stem cells [28]. The C3H10 cell lines were obtained from the cell bank of Chinese Academy of Sciences, Shanghai.

2.2. Experimental protocols

The rats were weighed every 2 weeks and underwent oral glucose tolerance tests (OGTT) after a 12 h fasting. Diabetes was diagnosed (Shanghai Shrek Experimental Animal Co., Ltd., Shanghai, China) as fasting blood glucose (0 min) ≥ 7.0 mmol/L twice, or 120 min blood glucose >11.1 mmol/L.

All GK rats were diagnosed with diabetes at the age of 13 weeks, and detailed blood glucose data were shown in Supplementary Table S2 and Figure S1. At the age of 21 weeks, the GK rats were assigned to groups without (GK; $n = 10$) or with 200 mg/kg/day metformin administered via oral gavage (Sino-US Shanghai Bristol-Myers Squibb Pharmaceutical Co., Ltd., Shanghai, China) for 20 weeks (GK + Met; $n = 8$) and 16 Wistar rats were served as healthy controls. The rats were sacrificed at the age of 41 weeks.

All rats were subcutaneously injected with 10 mg/kg calcein (a bone formation surface labeling reagent, purchased from Sigma–Aldrich Corp., St. Louis, MO, USA) on days 3, 4, 13, and 14 before sacrificed. Twenty weeks after the first treatment, the rats were sacrificed by cardiac puncture under anesthesia at the end of the experiments.

2.3. Serum biomarkers

Rat serum was collected and stored at -80°C . Serum ALP, OCN, carboxy-terminal cross-linking telopeptide of type 1 collagen (CTX-1), calcium (Ca), superoxide dismutase (SOD), tartrate-resistant acid phosphatase (TRAP), phosphate (P), malondialdehyde (MDA), GSP, cholesterol (CHO), low-density lipoprotein (LDL), and INS were detected using the commercial kits (Nanjing Jian Cheng Bioengineering Institute, Jiangsu, China) as described by the manufacturer.

2.4. Micro-computed tomography (μCT) assessment

The left proximal tibiae of rats were harvested at the endpoint and the samples were scanned using a Viva CT 40 $\mu\text{-CT}$ system (Scanco Medical, Zurich, Switzerland) with the scanning settings as follows: 70 kVp; 114 μA ; 8 W; integration time, 200 ms; and gaussian filter with sigma 0.8, support 1. A region of interest (ROI) in the proximal tibial metaphysis (PTM) for μCT analysis was set in the region of 1–3 mm distal to the growth plate–epiphyseal junction. Cortical bones were excluded. Three-dimensional (3D) parameters of trabecula were calculated and the 3D images were generated using Scanco system build-in software. Bone mineral density (vBMD, mg/cm^3), trabecular number (Tb.N, $1/\text{mm}$), bone volume (BV, mm^3), tissue volume (TV, mm^3), bone volume/tissue volume (BV/TV, %), connectivity density (Conn.D, $1/\text{mm}^3$), trabecular separation (Tb.Sp, mm), and trabecular thickness (Tb.Th, mm) were acquired by build-in software calculation.

2.5. Bone histomorphometry

The samples of proximal metaphysis of the right tibia and the fourth lumbar vertebra were collected and prepared for undecalcified sections. Samples were prepared for frontal sections of 5 and 8 μm . The slices of 5 μm were stained with Goldner trichrome staining for static histomorphometry analysis, and the 8 μm unstained slices were used for dynamic histomorphometry analysis. As to the midtibial diaphyseal cortical bone, cross sections of the tibial shaft (TX) were prepared and ground to a thickness of 20 μm for histomorphometric analysis. The quantitative analysis of bone histomorphometry was performed by using a semi-automatic digitizing image analysis system (Osteometrics, Inc.,

Decatur, GA, USA). The parameters of bone histomorphometry were chosen and calculated according to the Nomination Committee of Histomorphometry of the American Society of Bone and Mineral Research recommendation [29]. Ob.S (osteoblast surface, mm^2), Oc.S (osteoclast surface, mm^2), BS (bone surface, mm^2), MAR (mineral apposition rate, $\mu\text{m}/\text{d}$), BFR (bone formation rate, $\mu\text{m}/\text{d}$), Ct.Ar (cortical bone area, mm^2), E-L.Pm (endocortical single-labeled surface ratio in bone surface, %), P-MAR (periosteal mineral apposition rate, $\mu\text{m}/\text{d}$), P-BFR (periosteal bone formation rate, $\mu\text{m}/\text{d}$) were calculated as previously described [30, 31].

2.6. Biomechanical properties

We assessed the mechanical properties (three-point bending tests) of the right femurs using a Lloyd LR5K Plus material testing system (Ametek GmbH, Meerbusch, Germany). Each femur was placed on two stents 20 mm apart and a downward load was applied to the specimen at the midpoint of the two stents, causing the anterior and posterior surfaces of the femur to be respectively under compression and tension. The structural strength of each specimen was determined as maximum fracture load and yield load, as well as stiffness were calculated from load–displacement diagrams.

2.7. Histology

The samples of pancreas and gastrocnemius muscle were embedded in paraffin, sectioned, and stained with Hematoxylin-Eosin (HE) Stain Kit (G1120, Solarbio, China) at the endpoint for histology analysis.

2.8. Quantitative reverse transcription-PCR (RT-PCR)

Total RNA of gastrocnemius muscles was obtained by TRIzol assay (Thermo Fisher Scientific Inc., Waltham, MA, USA). Total RNA of C3H10 cells was collected by using TRIzol assay (Takara Bio Inc.) The total RNA was used to prepare complementary DNA by using reverse transcriptase kits (RR036A, Takara Bio Inc., Kusatsu, Japan) according to the manufacturer's instructions. The relative gene expression of Ubc, ALP, OCN, RAGE, STAT1, RUNX2 and Col1a1 were analyzed by using SYBR Green real-time PCR kits (SYBR® Premix Ex Taq™ II, RR820A; Takara Bio Inc.) and ABI 7500 Fast Real-Time PCR system (Applied Biosystems Life Technologies, Foster City, CA, USA). Expression of the relative gene was further normalized to that of GAPDH. Relative gene expression was quantified using the comparative threshold cycle ($2^{-\Delta\Delta C_t}$) calculation. The PCR reaction conditions were set as: 95 °C for 30 s, followed by 40 cycles of 95 °C for 5 s, and 60 °C for 34 s. Supplementary Table S2 shows the synthesized real-time PCR primers.

2.9. Cell viability

C3H10 cells were incubated without or with various concentrations of metformin in 96-well plates for 24, 48, and 72 h. The culture medium was replaced with fresh medium every two days, and cell viability was quantified using Cell Counting Kit-8 assay (C0038, Beyotime, Shanghai, China).

2.10. Osteogenic induction

Osteogenic differentiation of C3H10 cells was induced in Dulbecco's modified Eagle medium (DMEM, C11995500BT, Gibco) containing 50 μM ascorbic acid (1043003, sigma), 10 mM β -glycerophosphate (G9422, sigma), 100 nM dexamethasone (D4902, sigma) and 10% fetal bovine serum (10099–141, Gibco). The experiment group setting comprised healthy control cells (CON; incubated in complete medium) and cells incubated in osteogenic induction medium (OIM), OIM containing 35 mg/mL glucose (OIM + GH), or OIM containing 35 mg/mL glucose and 100 μM metformin (OIM + GH + MET).

2.11. Alkaline phosphatase staining

C3H10 cells were incubated in 12-well plates. The culture medium was replaced with fresh medium every two days for seven days of incubation, then ALP was detected using Alkaline Phosphatase Assay Kit (P0321S, Beyotime, Shanghai, China).

2.12. Network pharmacological prediction

We predicted targets of metformin using PharmMapper and Swiss target prediction databases and duplicate target genes were deleted. Disease-related targets were searched using the keywords, "Osteoporosis" and "T2DM" in the GeneCards, OMIM, DrugBank, and DisGenet databases, then duplicate target genes were deleted. We applied Venny 2.1.0 to intersect drug and disease targets. The intersectional targets were imported into the STRING database to determine protein intersectional relationships, and the protein–protein interaction (PPI) network was obtained using Cytoscape software. We set the node size and color intensity to reflect the degree value using the Generate style from the statistics tool in Cytoscape software, then filtered the top ten intersectional targets.

2.13. Western blotting

The cell samples were lysed in radioimmunoprecipitation assay (RIPA, P0013C, Beyotime, Shanghai, China) buffer on ice. The protein samples were collected by centrifugation at $10,000\times g$ at 4 °C for 10 min. Proteins (30 mg/sample) were prepared for SDS-PAGE. Protein samples were then transferred to polyvinylidene fluoride (PVDF, FFP77, Beyotime, Shanghai, China) membranes. The membranes were then incubated with primary antibodies overnight at 4 °C. Osterix (ab209484), RAGE (ab216329), JAK2 (ab108596), p-JAK2 (ab32101), STAT1 (ab92506), p-STAT1 (ab109461) were used at a concentration of 1:1,000, and GAPDH (A01020) was used as control at a concentration of 1:2000 (all antibodies were obtained from Abcam, Cambridge, UK), and the protein membranes were incubated with goat anti-rabbit IgG (A21020 Abbkine, Wuhan, China, concentration 1:5000) for 1 h at 37 °C. The immunoreactive bands were visualized using a FluorChem® Q Imaging System (ProteinSimple, Santa Clara, CA, USA) and the protein expression was quantified by Image J software and normalized to GAPDH (National Institutes of Health, Bethesda, MD, USA).

2.14. Statistical analysis

All experimental data were statistically analyzed using GraphPad Prism 8.0/SPSS 19.0 software (IBM Corp., Armonk, NY, USA) with one-way ANOVA. Results are expressed as means \pm standard deviation ($X \pm s$), and differences were considered statistically significant at $P < 0.05$.

3. Results

3.1. GK diabetic rats developed significant bone loss and bone quality deterioration

The GK rats had significant decreased bodyweight and higher serum glucose levels than the wild-type (WT) controls (Fig. 1A and B). Biochemical results indicated significantly decreased OCN and significantly increased TRAP, CTX-1, and ALP levels in GK rats compared with healthy controls. Serum levels of MDA, CHO, INS, and GSP were significantly increased, whereas SOD, low-density lipoprotein-cholesterol (LDL-C), and phosphorus (P) were significantly decreased in GK rats compared with healthy controls (Fig. 1C). The μ -CT results indicated a significantly decreased trabecular BV/TV ratio accompanied by significant deterioration in bone geometry and microstructure parameters (trabecular separation, Conn-D, trabecular number, vBMD, and trabecular thickness) in GK rats compared with controls (Fig. 2). The histomorphological

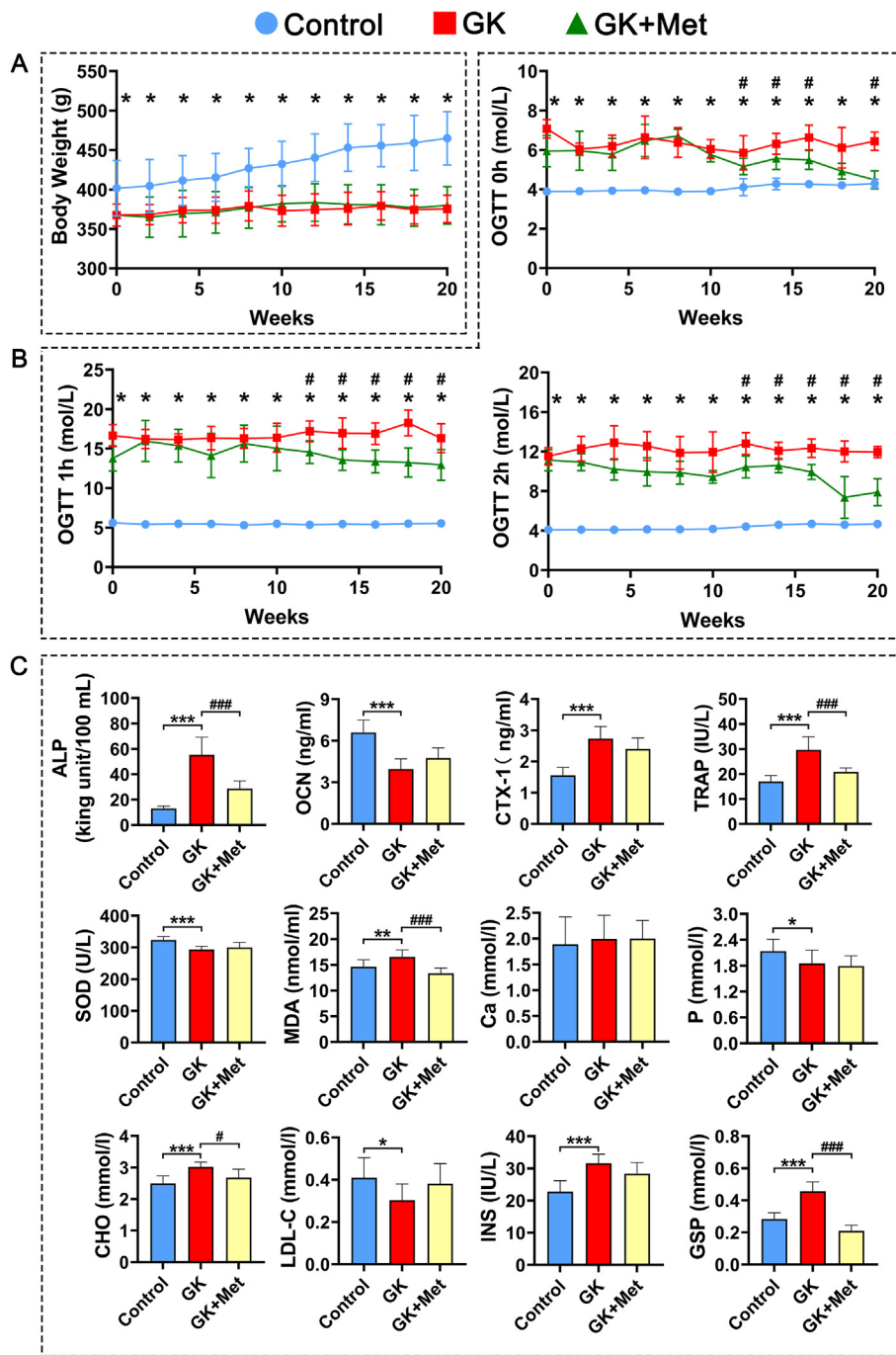


Fig. 1. Body weight, glucose tolerance and serum biochemical markers in GK rats with T2DM treated with metformin (A) Body weight of GK rats with T2DM treated with metformin (B) Effects of metformin on serum glucose determined by oral glucose tolerance tests (OGTT) in GK rats with T2DM (C) Serum biochemical markers in GK rats with T2DM treated with metformin. Note: Vs. Control * $P < 0.05$, ** $P < 0.01$, *** $P < 0.001$; vs. GK # $P < 0.05$, ## $P < 0.01$, ### $P < 0.001$. Values are presented as mean \pm SD.

results revealed significantly deteriorated bone static parameters (trabecular area ratio, thickness, trabecular, and separation) in GK rats (Fig. 4). The bone formation rate, bone formation parameters of mineralization, and mineral apposition rate were also significantly decreased in the GK rats (Fig. 3). Trabecular and cortical bone was deteriorated in GK rats (Fig. 3). Similar histomorphometric results were found in the lumbar spine and PTM among groups (Figs. 3E and 4). In terms of bone mechanical properties, apparent material strength determined as maximum, elastic, and fracture loads decreased by 18.5%, 15.6%, and 17.1%, respectively and structural strength determined as stiffness significantly decreased by 12.3% in GK diabetic rats compared to control rats (Fig. 4E). The histological results also revealed significant pathological changes in the gastrocnemius muscle and pancreatic islets with a lower islet cell density in GK diabetic rats compared with controls. The

gastrocnemius weight and muscle fibers number both decreased significantly, whereas Ubc gene expression was increased in GK diabetic rats compared with controls (Fig. 5).

3.2. Metformin suppressed bone resorption, restored bone formation, and increased bone and muscle quality in GK diabetic rats

The serum biomarker results showed increased OCN and significantly decreased TRAP and ALP levels in GK rats treated with/without metformin (Fig. 1C). Metformin also decreased the elevated levels of MDA, CHO, GSP, serum glucose, and INS in GK diabetic rats (Fig. 1C). The μ -CT analysis showed that metformin significantly increased vBMD, Conn-D, and trabecular BV/TV compared with that of untreated GK rats (Fig. 2). Metformin also increased the mineral apposition rate, bone

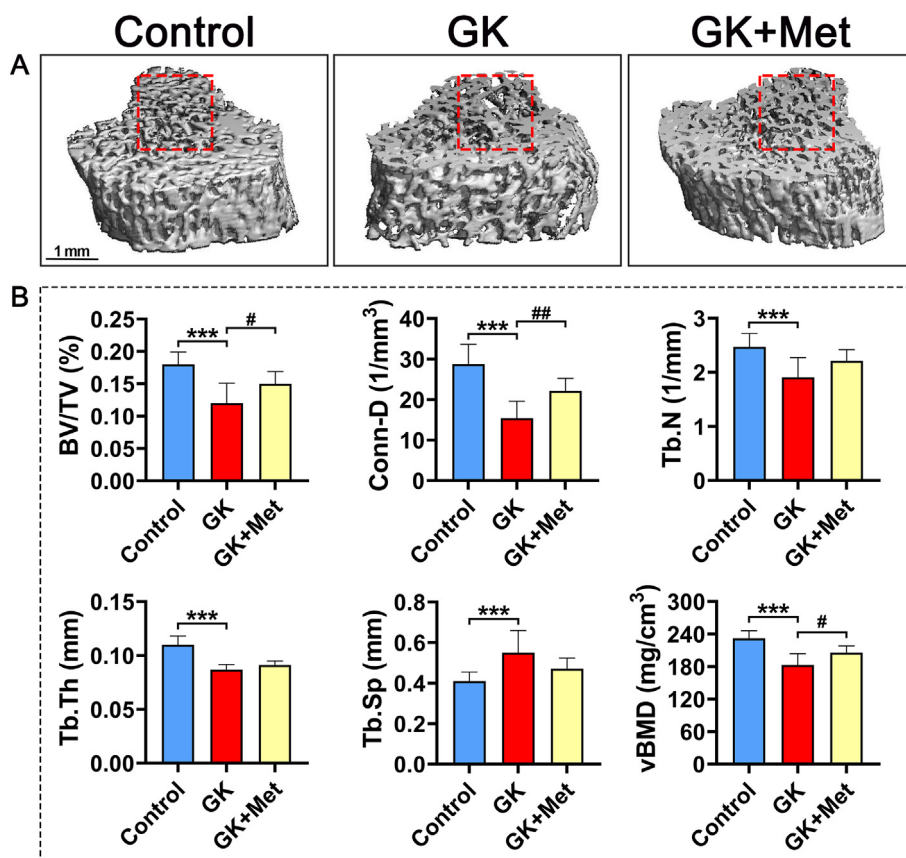


Fig. 2. Representative images of μ -CT of PTM in GK diabetic rats treated with metformin (A) Representative 3D μ -CT images of proximal tibial metaphysis (PTM) from GK rats with T2DM treated with metformin (B) Analysis of μ -CT images in (A). Note: Vs. Control * $P < 0.05$, ** $P < 0.01$, *** $P < 0.001$; vs. GK # $P < 0.05$, ## $P < 0.01$, ### $P < 0.001$. Values are presented as mean \pm SD.

formation parameters, and bone formation rate in corticoid and trabecular bones (Fig. 3A–D). Histomorphometry results of the lumbar spine demonstrated similar trend compared to PTM (Fig. 3E). Bone histomorphometry results revealed that metformin significantly improved the trabecular area, thickness, number, and separation compared to untreated GK rats (Fig. 4A–D). Bone biomechanical data demonstrated that maximum, elastic, and fracture load significantly increased by 14.5%, 9.7%, and 14.0%, respectively and stiffness also increased by 11.3% in the OIM + GH + MET group compared with that in the GK group (Fig. 4E). Additionally, the increased Ubc gene expression as well as decreased muscle fiber number in the gastrocnemius muscle were significantly alleviated in the OIM + GH + MET group. Pancreatic islet cell density was increased in the OIM + GH + MET group (Fig. 5).

3.3. Metformin reversed osteogenesis inhibition in a cell model of high glucose *in vitro*

Metformin (100 μ M) treatment for 48 h significantly increased cell viability of C3H10 cells (Fig. 6A). The results of ALP staining suggested that high glucose condition significantly inhibited ALP activity, but metformin could reverse the inhibitory effect on osteogenesis caused by high glucose (Fig. 6B). The network pharmacology results predicted 34 intersectional targets of metformin in the treatment of T2DM-OP diseases, of which 32 comprised a protein interaction network. According to its degree value, STAT1, which is closely related to glucose and bone metabolism, ranked the 6th in the significant differential genes (Fig. 7A–D). The AGE-RAGE signaling pathway is closely related to glucose metabolism, and STAT1 is one of the downstream targets in the AGE-RAGE signaling cascades (Fig. 7E). The results of RT-qPCR suggested that the high concentration of glucose significantly inhibited the

gene expression of ALP, Col1a1, OCN, and RUNX2, while increasing RAGE and STAT1 *in vitro*. In contrast, metformin significantly increased the gene expression of ALP, OCN, Col1a1, and RUNX2 and significantly decreased that of RAGE and STAT1 (Fig. 7F). Therefore, the RT-qPCR data confirmed that STAT1 plays an important role in the regulation of metformin in a cell model of diabetes *in vitro*. The western blotting results suggested that the high concentration of glucose significantly inhibited Osterix protein expression while increasing those of RAGE, p-JAK2, and p-STAT1. In contrast, metformin stimulated Osterix protein expression while suppressing that of RAGE, p-JAK2, and p-STAT1 (Fig. 7G–H).

Our data revealed that metformin effectively improves bone and muscle mass in GK rats with diabetes *in vivo* and reverse osteogenesis inhibition in a high-glucose cell model *in vitro* by regulating the RAGE-JAK2-STAT1 signaling axis.

4. Discussion

The present findings in this study showed that GK rats had higher levels of INS, serum glucose, and GSP as well as degenerative changes in the pancreas, which is a cardinal symptom of T2DM. We found that T2DM significantly increased bone resorption, impaired bone formation, and further induced the degeneration of biomechanical properties and bone microarchitecture. We also found that the tibia and lumbar vertebrae deteriorated significantly in GK rats. In addition, T2DM causes increased muscle loss and degradation, which further impairs the musculoskeletal system in GK rats. Furthermore, the osteogenic differentiation of C3H10 cells was significantly inhibited by incubation with high glucose medium.

Metformin is not only a conventional antidiabetic medicine that decreases blood glucose, but it also reduces fracture risk in patients with

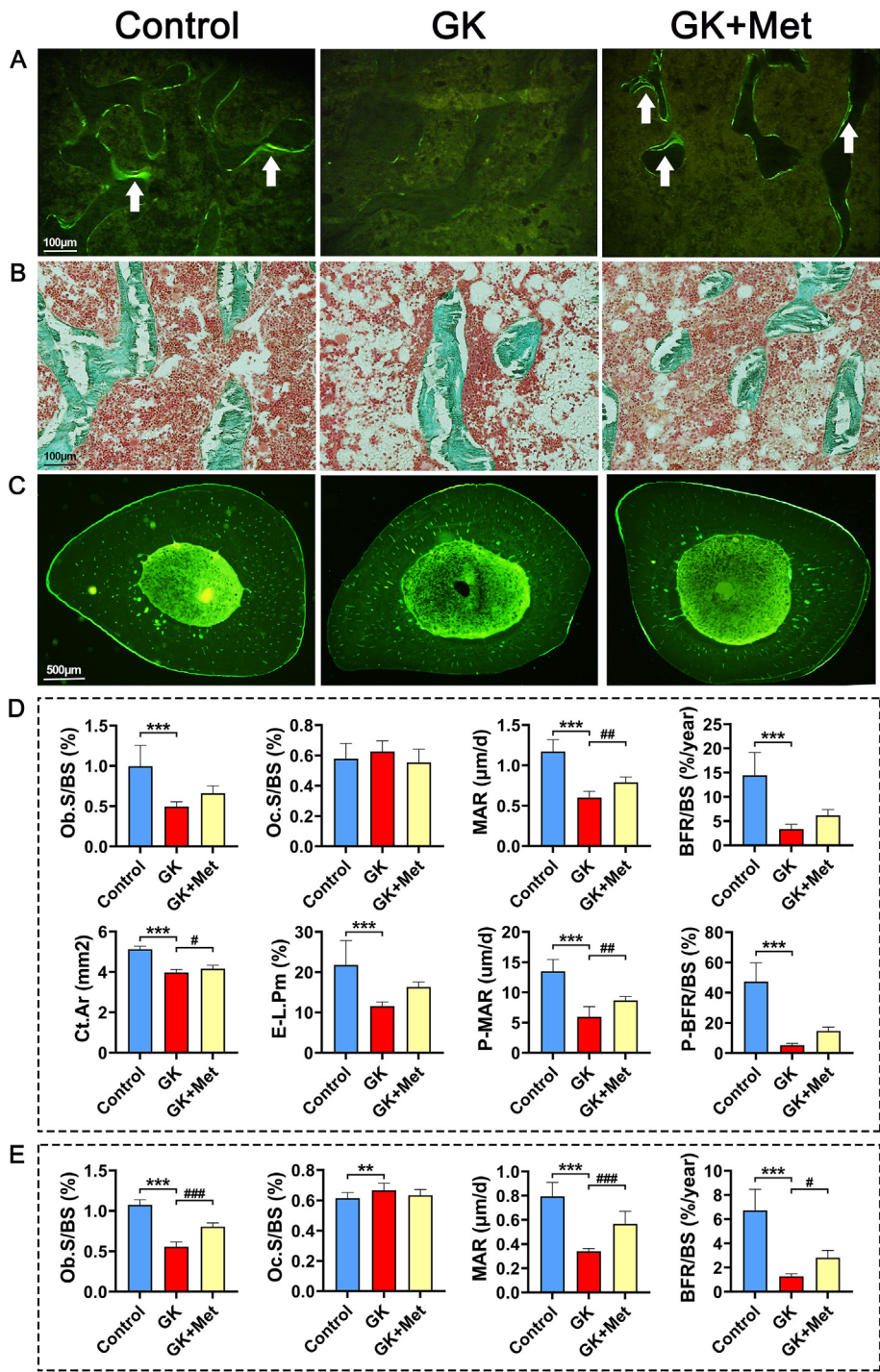


Fig. 3. Representative images of PTM and TX histomorphometry in GK rats treated with metformin (A) Fluorescent micrographs of PTM (undecalcified sections with calcein labeling) (B) Micrographs of PTM (undecalcified sections with Goldner trichrome staining (C) Representative fluorescent micrographs of tibial shaft (TX) (undecalcified sections with calcein labeling) (D) histomorphometric parameters of proximal tibial metaphysis (PTM) and tibial shaft (TX) (E) histomorphometric parameters of lumbar vertebrae. Note: Vs. Control * $P < 0.05$, ** $P < 0.01$, *** $P < 0.001$; vs. GK # $P < 0.05$, ## $P < 0.01$, ### $P < 0.001$. Values are presented as mean \pm SD.

diabetes [32] and improves bone loss in normal adult women [33]. Previous studies have shown that metformin increases the bone mass of glucocorticoids [34], improves ovariectomized induced osteoporosis [35] and bone microstructure [35], and stimulates trabecular and cortical bone formation [34]. In our study, metformin significantly decreased blood glucose and GSP levels and attenuated pancreatic damage in GK rats with T2DM compared with untreated GK rats. Metformin increased trabecular bone mass in both the tibia and lumbar vertebrae, promoted bone formation, and resulted in significant improved bone biomechanical properties compared to untreated GK rats. In addition, metformin attenuated muscle loss and degeneration in GK rats. All these effects help to reduce the risk of fractures associated

with diabetes. Metformin also stimulated the cell viability of mesenchymal stem cells and alleviated the inhibitory effect of high glucose on osteogenic differentiation. To further elucidate the potential signaling cascade of metformin in bone metabolism, we used network pharmacology to predict potential targets involved in the metformin regulation cascade. We identified STAT1 as a likely target protein involved in the metformin regulation. We then assessed STAT1 and STAT1 upstream signaling molecules using C3H10 cells incubated under a high glucose concentration. We found that the effects of metformin on bone metabolism are closely associated with suppression of the RAGE-JAK2-STAT1 signaling axis.

Long-term hyperglycemia in T2DM leads to the accumulation of AGEs

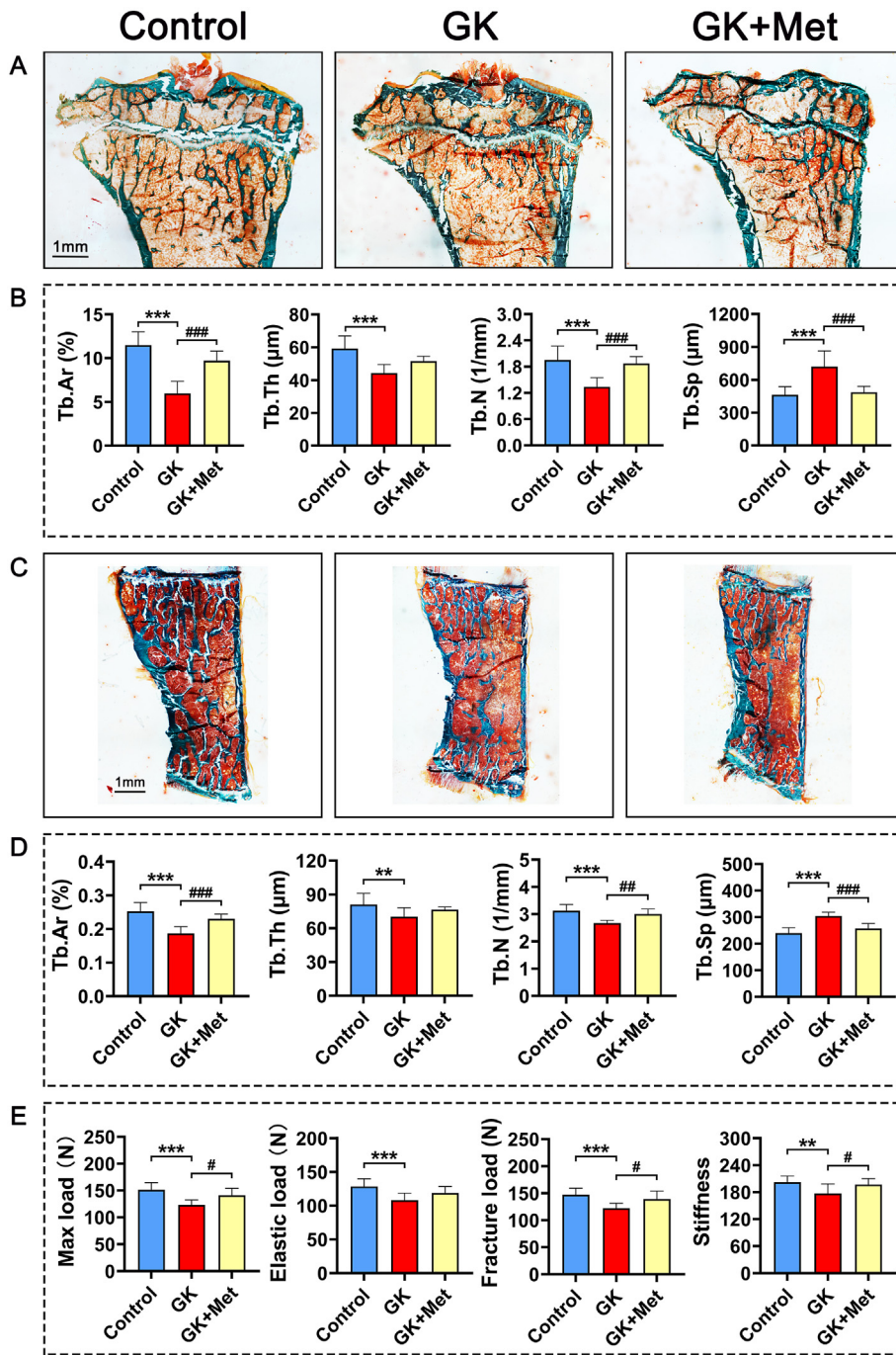


Fig. 4. Effects of metformin on PTM, lumbar vertebrae and bone biomechanical properties in GK diabetic rats (A) Representative micrographs of PTM histomorphometry (undecalcified sections with Goldner trichrome staining) (B) Effects of metformin on static parameters of right upper tibia cancellous bone in GK rats (C) Representative micrographs of lumbar vertebrae (undecalcified sections with Goldner trichrome staining). Effects of metformin on (D) static parameters of lumbar cancellous bone and (E) biomechanical properties of bone in GK rats. Note: Vs. Control * $P < 0.05$, ** $P < 0.01$, *** $P < 0.001$; vs. GK # $P < 0.05$, ## $P < 0.01$, ### $P < 0.001$. Values are presented as mean \pm SD.

that are closely associated with deteriorating bone quality [36]. AGEs can induce apoptosis of osteoblasts through interaction with its receptor (RAGE) [37]. In addition, AGEs can activate the JAK2-STAT1 signaling pathway and produce more negative biological effects [38,39]. AGEs can also induce the production of reactive oxygen species (ROS) [40] and cause diabetes-related bone injury by upregulating STAT1 expression [39,41]. The RAGE-JAK2-STAT1 signaling axis is involved in glucose and bone metabolism, as STAT1 is a cytoplasmic attenuator of Runx2 in the transcriptional cascade of osteoblast differentiation [42]. Inhibiting STAT1 accelerates fracture healing [43] and promotes osteoblast proliferation and differentiation [44]. In contrast, activated STAT1 expression in mouse mesenchymal stem cells decreases osteogenic differentiation [45]. Our results showed that the osteogenic differentiation of C3H10 cells incubated with high glucose was significantly inhibited, whereas the

protein expression of RAGE, p-JAK2, and p-STAT1 was increased significantly. Metformin alleviated the osteogenic inhibition of C3H10 cells induced by high glucose, promoted the expression of ALP, OCN, RUNX2, Col1a1 and Osterix, and inhibited the RAGE-JAK2-STAT1 signaling axis. Metformin decreased MDA and increased SOD in serum of GK rats, and also decrease STAT1 expression, which helped to relieve oxidative stress and further alleviated diabetes-induced osteoporosis. Therefore, the potential mechanism of metformin on bone metabolism in T2DM might be associated with inhibiting the RAGE-JAK2-STAT1 signaling axis.

Although JAK-STAT signal axis was reported that involved in the effects of Metformin, the JAK-STAT signal axis mostly reported in nonskeletal tissues. Metformin provided cardioprotective effect through JAK/STAT pathway for the prevention of diabetic cardiomyopathy [46]

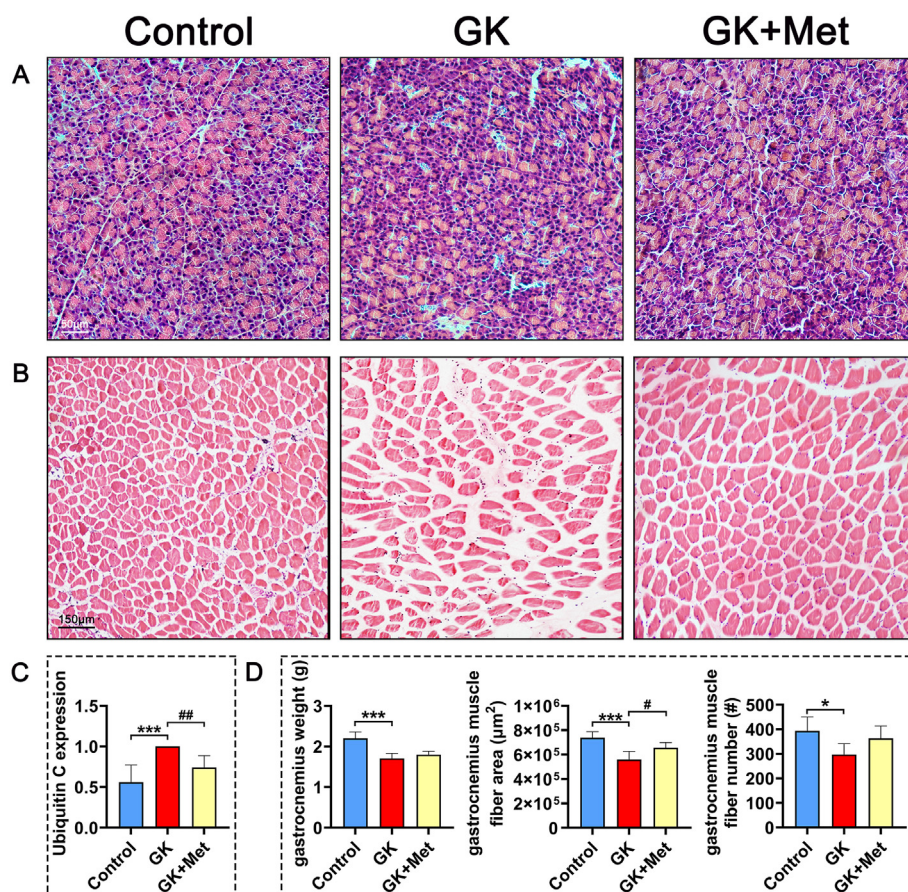


Fig. 5. Pathological findings of pancreas and gastrocnemius muscle in GK rats with T2DM treated by metformin. Representative images of (A) pancreas and (B) gastrocnemius muscle histologically stained with HE (C) Expression of ubiquitin C in gastrocnemius muscle (D) Analysis of gastrocnemius muscles. HE, hematoxylin and eosin. Note: Vs. Control * $P < 0.05$, ** $P < 0.01$, *** $P < 0.001$; vs. GK # $P < 0.05$, ## $P < 0.01$, ### $P < 0.001$. Values are presented as mean \pm SD.

(heart cells/tissue, JAK2-STAT3). Metformin also reduced the dermal thickness and fibrosis in systemic sclerosis by regulating JAK/STAT pathway. In addition, previous studies reported STAT1 mainly focuses on diabetic nephropathy [47,48]. High glucose can activate the JAK/STAT pathway in glomerular mesangial cells [49,50], however, there are few studies related to bone metabolism. Currently, seldom studies revealed that metformin regulates bone metabolism through JAK/STAT signal axis.

In our study, we specifically demonstrated metformin regulates stem cell osteogenic differentiation through JAK/STAT signal axis, especially in high sugar microenvironment, which RAGE initiated the RAGE-JAK2-STAT1 signaling cascade. Previous studies only reported metformin regulates JAK2-STAT3 in heart tissue, while we found that metformin regulated JAK2-STAT1 in bone. These results suggest that metformin may regulate different STAT sub-type protein in different tissues. In this study, we first used network pharmacology prediction analysis to screen the potential signal axis of metformin on bone metabolism of stem cell, we found that high sugar microenvironment may induce RAGE over expression and then conducted signal to JAK2-STAT1 axis, and metformin may block this signal cascade and provide beneficial effects on bone metabolism. Therefore, we then verified this potential mechanism by using qPCR and Western blot assay. Our results demonstrated metformin did suppress RAGE-JAK2-STAT1 signal axis, and therefore increased the osteogenic differentiation of MSCs in a high-sugar microenvironment. Previous studies did not clearly reveal such signal axis before. RAGE-JAK2-STAT1 play an important role in the metformin regulation of promoting stem cell osteogenic differentiation in diabetes. *In vivo* study, several different assays (micro-CT, histomorphometry, serum elisa, and histology) were using to evaluate metformin treatment for diabetes-

induce osteoporosis rats. We showed that metformin treatment for diabetic rats could attenuate bone osteopenia, improve bone microstructure, and stimulate bone formation in GK diabetic rats.

Bone remodeling is a complex process that involve different bone cells [51]. Previous studies demonstrated metformin not only promoted osteogenic differentiation of stem cells, but also regulate gene and protein expression in osteoblasts and osteoclast precursors, thereby attenuated osteopenia [52]. In osteoblasts, metformin can promote AMPK [53], BMP2 [53], IGF-1 [54] and e/iNOS expression [55], thereby increasing the activity of ALP in osteoblasts, promoting calcium deposition with increased mineralized nodules for bone formation. What's more, metformin promoted OPG expression while decreased RANKL expression in mouse calvarial osteoblasts and osteoblast cell line MC3T3-E1 in a dose-dependent manner [52]. In addition, metformin inhibits osteoclast activation by down-regulating the expression of inflammatory factors [56], p-ERK [57], RANKL [58], and macrophage colony-stimulating factor (M-CSF) [58]. Furthermore, metformin also down-regulated E2F1 expression and inhibited autophagy of osteoclast precursors, which in turn to inhibit osteoclastogenesis and reduce bone loss in ovariectomized mice [59]. Besides, metformin also protects against homocysteine-induced apoptosis of osteocytic MLO-Y4 cells by regulating the expression of NADPH oxidase 1 (Nox1) and Nox2 [60].

In this study, we focus on how metformin regulates the osteogenic differentiation of stem cells in hyperglycemia condition, and we found that RAGE-JAK2-STAT1 signal axis plays an important role in the metformin regulation process. Our data provide comprehensive evidence that metformin could attenuate bone osteopenia in diabetes rats and stimulate bone formation *in vivo*. The results were confirmed by different assays, including micro-CT, histomorphometry, serum elisa, and

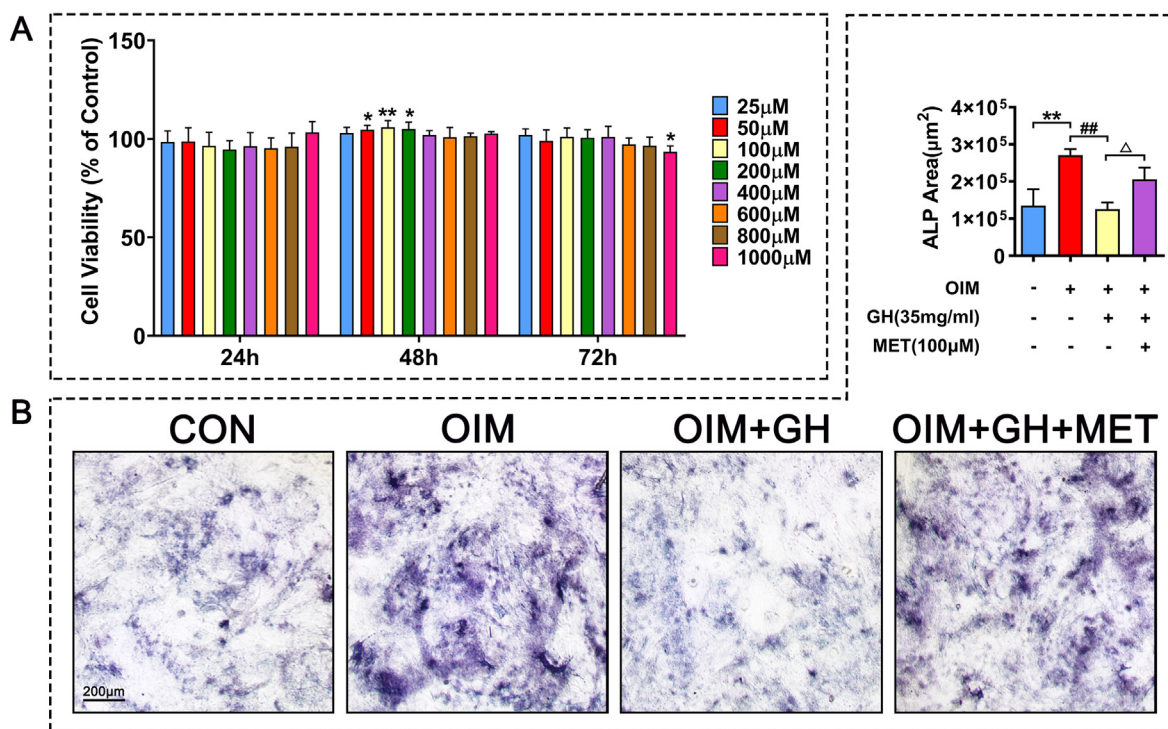


Fig. 6. Effects of metformin on osteogenic differentiation of C3H10 cells induced by high glucose (A) Cell viability of C3H10 cells incubated with metformin for 24, 48, and 72 h (B) Effects of metformin on ALP activity in C3H10 cells induced by high glucose. Note: Vs. Control * $P < 0.05$, ** $P < 0.01$, *** $P < 0.001$; vs. OIM # $P < 0.05$, ## $P < 0.01$, ### $P < 0.001$; vs. OIM + GH $\Delta P < 0.05$, $\Delta\Delta P < 0.01$, $\Delta\Delta\Delta P < 0.001$. Values are presented as mean \pm SD.

histology analyses. We also noticed that our study has limitations, the specific mechanism of metformin in the regulation of glucose metabolism and bone metabolism still needs to be further explored.

Sarcopenia usually refers to the loss of skeletal muscle function and quality related to aging. A meta-analysis of 16,800 patients with T2DM found that metformin helped to alleviate sarcopenia [61]. Metformin can enhance skeletal muscle function through promoting skeletal muscle cell differentiation and myotube maturation [62]. Metformin partially enhances peroxisome proliferator-activated receptor-gamma coactivator-1 alpha (PGC-1 α) expression and mitochondrial biogenesis through AMPK phosphorylation in the skeletal muscle and improve INS resistance [63]. In addition, activated PGC-1 α further downregulates forkhead box O3 (FOXO3) and leads to the suppression of muscle atrophy [64]. Metformin treatment also inhibits the expression of Ubc, which is beneficial for protecting muscle function [65]. Consistent with the above results, we results demonstrated that metformin significantly increased the weight of the gastrocnemius muscle and inhibited Ubc expression in GK rats with T2DM, suggesting that metformin suppresses muscle degradation and improves muscle quality. Although our study found that metformin alleviated the loss of gastrocnemius muscle weight and muscle fibers in GK rats caused by T2DM, which may be related to the inhibition of Ubc expression, future studies are needed to provide more evidence and further elucidate the specific mechanism.

In conclusion, metformin attenuated osteopenia and muscle degeneration in GK rats with T2DM and alleviated osteogenesis inhibition caused by excessive glucose. The effects of metformin on diabetes-induced osteopenia might be associated with suppression of the RAGE-JAK2-STAT1 signaling axis. Clinically, metformin is mainly used to reduce high blood glucose levels in patients with type 2 diabetes, and our study provided a specific and comprehensive potential mechanism for how metformin regulates osteogenic differentiation of stem cell and interfered bone metabolism in diabetes, and further verified the metformin effects *in vivo*. Our study may provide a research basis for the clinical research of metformin in diabetic osteoporosis.

Funding information

This research was funded by grants from the National Natural Science Foundation of China (No. 81703584), The regional joint fund of Natural Science Foundation of Guangdong Province (No. 2020B1515120052), Guangdong Province Natural Science Foundation of China (No. 2022A1515220166, 2017A030310614, 2021A1515010975), Discipline construction project of Guangdong Medical University (No. 4SG22002G, 4SG21156G, and CLP2021B012), the Discipline Construction Fund of Central People's Hospital of Zhanjiang (No. 2022A09), Special Funds for Scientific Technological Innovation of Undergraduates in Guangdong Province (No. pdjh2022a0214), the Science and Technology Foundation of Zhanjiang (No. 2022A01099), Guangdong medical university research fund: FZZM05.

Authorship

Category 1

Conception and design of study: Y.Z. Liu, L. Cui, Acquisition of data: R. Lin, B.L. Xu, Z.Q. Ye, Y. Gao, H.P. Fang, J.T. Song, D.H. Liang, L.N. Liu, Z.L. Hu, M. Zhang, J.S. Wei, F.F. Deng, X.X. Zhong, analysis and/or interpretation of data: R. Lin, Z.Q. Ye, Y. Gao, H.P. Fang, J.T. Song, D.H. Liang, L.N. Liu, Z.L. Hu, M. Zhang, J.S. Wei, F.F. Deng, X.X. Zhong

Category 2

Drafting the manuscript: R. Lin, B.L. Xu, Z.Q. Ye, revising the manuscript critically for important intellectual content: Y.Z. Liu, L. Cui.

Category 3

Approval of the version of the manuscript to be published (the names of all authors must be listed): R. Lin, B.L. Xu, Z.Q. Ye, Y. Gao, H.P. Fang, J.T. Song, D.H. Liang, L.N. Liu, Z.L. Hu, M. Zhang, J.S. Wei, F.F. Deng, X.X. Zhong, L. Cui**, Y.Z. Liu*

Declaration of competing interest

The authors declare that they have no known competing financial

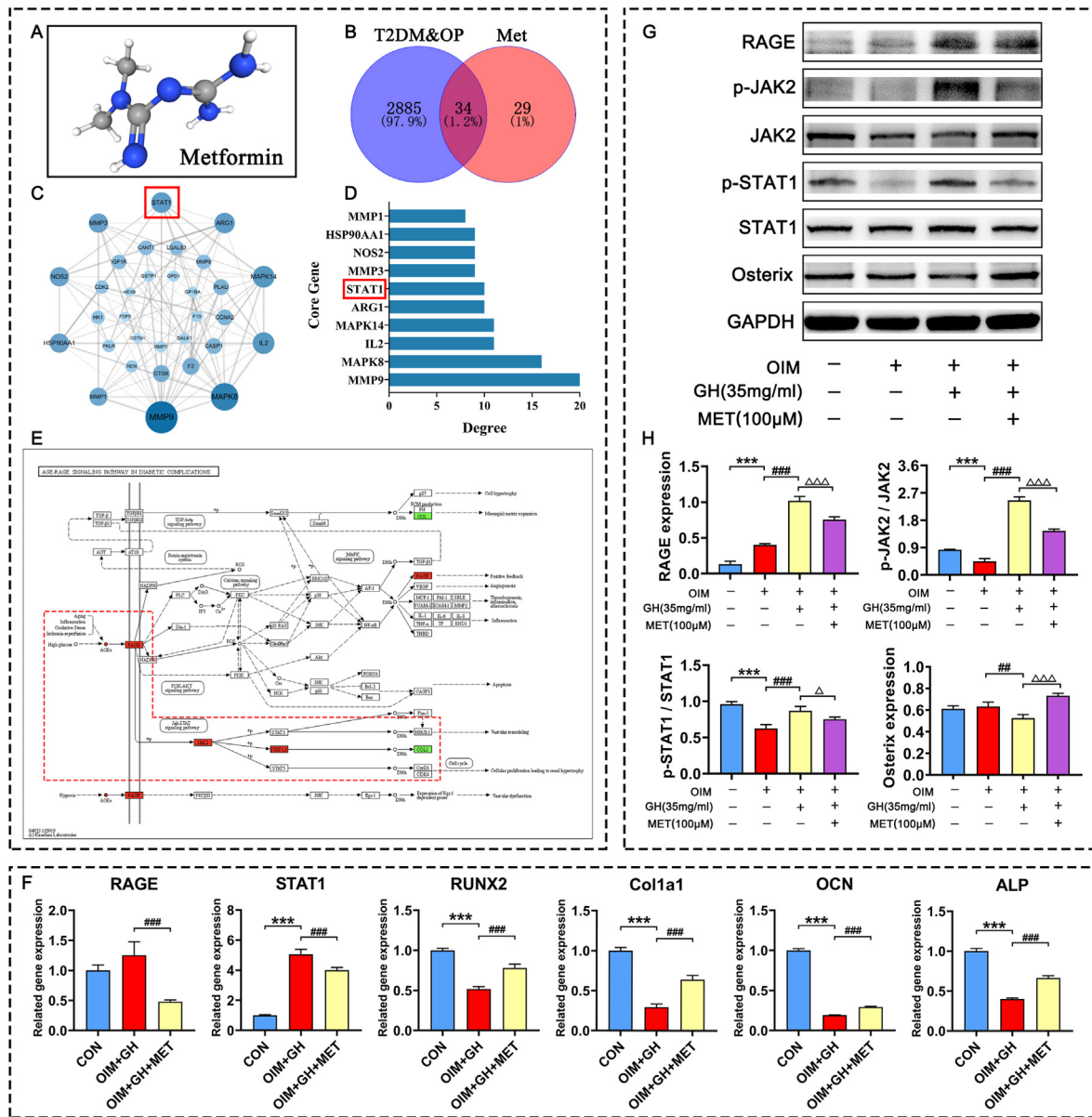


Fig. 7. Effects of metformin on osteogenic differentiation of C3H10 cells induced with high concentrations of glucose (A) Chemical structural of metformin (B) Wayne diagram of potential targets of metformin in the treatment of T2DM-OP disease (C) Protein interaction network of potential targets (D) Degree values of top ten potential targets (E) Gene expression of C3H10 cells induced by high glucose visualized in KEGG pathway of the RAGE-JAK2-STAT1 signal axis (F) RAGE, STAT1, RUNX2, Col1a1, OCN and ALP gene expression in C3H10 cells induced by high glucose determined by RT-qPCR (G) Western blots show effects of metformin on protein levels of RAGE, p-JAK2, JAK2, p-STAT1, STAT1 and Osterix in C3H10 cells induced by high glucose (H) Protein levels of RAGE, p-JAK2/JAK2, p-STAT1/STAT1 and Osterix. Note: Vs. Control **P* < 0.05, ***P* < 0.01, ****P* < 0.001; vs. OIM #*P* < 0.05, ##*P* < 0.01, ###*P* < 0.001; vs. OIM + GH Δ *P* < 0.05, $\Delta\Delta$ *P* < 0.01, $\Delta\Delta\Delta$ *P* < 0.001. Values are presented as mean \pm SD.

interests or personal relationships that could have appeared to influence the work reported in this paper.

Acknowledgements

All persons who have made substantial contributions to the work reported in the manuscript (e.g., technical help, writing and editing assistance, general support), but who do not meet the criteria for authorship, are named in the Acknowledgements and have given us their written permission to be named. If we have not included an Acknowledgements, then that indicates that we have not received substantial contributions from non-authors.

Appendix A. Supplementary data

Supplementary data to this article can be found online at <https://doi.org/10.1016/j.jot.2023.05.002>.

References

- [1] Ogurtsova K, Guariguata L, Barengo NC, Ruiz PL, Sacre JW, Karuranga S, et al. IDF diabetes Atlas: global estimates of undiagnosed diabetes in adults for 2021. *Diabetes Res Clin Pract* 2022;183:109118.
- [2] World Health O. *Global report on diabetes*. Geneva: World Health Organization; 2016.
- [3] Ma Q, Li Y, Li P, Wang M, Wang J, Tang Z, et al. Research progress in the relationship between type 2 diabetes mellitus and intestinal flora. *Biomed. Pharmacother. Biomed. Pharmacother.* 2019;117:109138.

- [4] Huang TW, Chen JY, Wu YL, Kao CC, Yeh SC, Lin YC. Alterations of bone markers in obese patients with type 2 diabetes after bariatric surgery: a meta-analysis and systematic review of randomized controlled trials and cohorts. *Medicine* 2021; 100(20):e26061.
- [5] Huang R, Wang H, Shen Z, Cai T, Zhou Y, Wang Y, et al. Increased glycemic variability evaluated by continuous glucose monitoring is associated with osteoporosis in type 2 diabetic patients. *Front Endocrinol* 2022;13:861131.
- [6] Cooper ID, Brookler KH, Crofts CAP. Rethinking fragility fractures in type 2 diabetes: the link between hyperinsulinaemia and osteofragilitas. *Biomedicine* 2021;9(9).
- [7] Catalfamo DL, Britten TM, Storch DL, Calderon NL, Sorenson HL, Wallet SM. Hyperglycemia induced and intrinsic alterations in type 2 diabetes-derived osteoclast function. *Oral Dis* 2013;19(3):303–12.
- [8] Sheweta SA, Khoshhal KI. Calcium metabolism and oxidative stress in bone fractures: role of antioxidants. *Curr Drug Metabol* 2007;8(5):519–25.
- [9] Giacco F, Brownlee M. Oxidative stress and diabetic complications. *Circ Res* 2010; 107(9):1058–70.
- [10] Karim L, Moulton J, Van Vliet M, Velie K, Robbins A, Malekipoor F, et al. Bone microarchitecture, biomechanical properties, and advanced glycation end-products in the proximal femur of adults with type 2 diabetes. *Bone* 2018;114:32–9.
- [11] Piccoli A, Cannata F, Strollo R, Pedone C, Leanza G, Russo F, et al. Sclerostin regulation, microarchitecture, and advanced glycation end-products in the bone of elderly women with type 2 diabetes. *J Bone Miner Res : Off. J. Am. Soc. Bone Mineral Res.* 2020;35(12):2415–22.
- [12] Vestergaard P. Discrepancies in bone mineral density and fracture risk in patients with type 1 and type 2 diabetes—a meta-analysis. *Osteoporos Int : a journal established as result of cooperation between the European Foundation for Osteoporosis and the National Osteoporosis Foundation of the USA* 2007;18(4): 427–44.
- [13] Janghorbani M, Van Dam RM, Willett WC, Hu FB. Systematic review of type 1 and type 2 diabetes mellitus and risk of fracture. *Am J Epidemiol* 2007;166(5):495–505.
- [14] Haentjens P, Magaziner J, Colón-Emeric CS, Vanderschueren D, Milisen K, Velkeniers B, et al. Meta-analysis: excess mortality after hip fracture among older women and men. *Ann Intern Med* 2010;152(6):380–90.
- [15] Bertram M, Norman R, Kemp L, Vos T. Review of the long-term disability associated with hip fractures, Injury prevention. *Journal of the International Society for Child and Adolescent Injury Prevention* 2011;17(6):365–70.
- [16] Farr JN, Khosla S. Determinants of bone strength and quality in diabetes mellitus in humans. *Bone* 2016;82:28–34.
- [17] Yamamoto M, Sugimoto T. Advanced glycation end products, diabetes, and bone strength. *Curr Osteoporos Rep* 2016;14(6):320–6.
- [18] Al-Hariri M. Sweet bones: the pathogenesis of bone alteration in diabetes. *J Diabetes Res* 2016;2016:6969040.
- [19] Qu B, He J, Zeng Z, Yang H, Liu Z, Cao Z, et al. MiR-155 inhibition alleviates suppression of osteoblastic differentiation by high glucose and free fatty acids in human bone marrow stromal cells by upregulating SIRT1. *Pflug Arch Eur J Physiol* 2020;472(4):473–80.
- [20] Zhai Z, Chen W, Hu Q, Wang X, Zhao Q, Tuexunying M. High glucose inhibits osteogenic differentiation of bone marrow mesenchymal stem cells via regulating miR-493-5p/ZEB2 signalling. *Journal of biochemistry* 2020;167(6):613–21.
- [21] Inzucchi SE, Bergenstal RM, Buse JB, Diamant M, Ferrannini E, Nauck M, et al. Management of hyperglycemia in type 2 diabetes, 2015: a patient-centered approach: update to a position statement of the American Diabetes Association and the European Association for the Study of Diabetes. *Diabetes Care* 2015;38(1): 140–9.
- [22] Shen M, Yu H, Jin Y, Mo J, Sui J, Qian X, et al. Metformin facilitates osteoblastic differentiation and M2 macrophage polarization by PI3K/AKT/mTOR pathway in human umbilical cord mesenchymal stem cells. *Stem Cell Int* 2022;2022:9498876.
- [23] Lei T, Deng S, Chen P, Xiao Z, Cai S, Hang Z, et al. Metformin enhances the osteogenesis and angiogenesis of human umbilical cord mesenchymal stem cells for tissue regeneration engineering. *Int J Biochem Cell Biol* 2021;141:106086.
- [24] Zhou Z, Tang Y, Jin X, Chen C, Lu Y, Liu L, et al. Metformin inhibits advanced glycation end products-induced inflammatory response in murine macrophages partly through AMPK activation and RAGE/NFκB pathway suppression. *J Diabetes Res* 2016;2016:4847812.
- [25] Tolosa MJ, Chuguransky SR, Sedlinsky C, Schurman L, McCarthy AD, Molinuevo MS, et al. Insulin-deficient diabetes-induced bone microarchitecture alterations are associated with a decrease in the osteogenic potential of bone marrow progenitor cells: preventive effects of metformin. *Diabetes Res Clin Pract* 2013;101(2):177–86.
- [26] Guest PC. Characterization of the goto-kakizaki (GK) rat model of type 2 diabetes. *Methods Mol Biol* 2019;1916:203–11.
- [27] Reznikoff CA, Brankow DW, Heidelberger C. Establishment and characterization of a cloned line of C3H mouse embryo cells sensitive to postconfluence inhibition of division. *Cancer Res* 1973;33(12):3231–8.
- [28] Pinney DF, Emerson Jr CP. 10T1/2 cells: an in vitro model for molecular genetic analysis of mesodermal determination and differentiation. *Environ Health Perspect* 1989;80:221–7.
- [29] Dempster DW, Compston JE, Drezner MK, Glorieux FH, Kanis JA, Malluche H, et al. Standardized nomenclature, symbols, and units for bone histomorphometry: a 2012 update of the report of the ASBMR Histomorphometry Nomenclature Committee. *J Bone Miner Res : Off. J. Am. Soc. Bone Mineral Res.* 2013;28(1):2–17.
- [30] Liu Y, Cui Y, Zhang X, Gao X, Su Y, Xu B, et al. Effects of salivianolate on bone metabolism in glucocorticoid-treated lupus-prone B6.MRL-Fas (lpr)/J mice. *Drug Des Dev Ther* 2016;10:2535–46.
- [31] Liu Y, Cui Y, Chen Y, Gao X, Su Y, Cui L. Effects of dexamethasone, celecoxib, and methotrexate on the histology and metabolism of bone tissue in healthy Sprague Dawley rats. *Clin Interv Aging* 2015;10:1245–53.
- [32] Tseng CH. Metformin use is associated with a lower risk of osteoporosis/vertebral fracture in Taiwanese patients with type 2 diabetes mellitus. *Eur J Endocrinol* 2021; 184(2):299–310.
- [33] Blümel JE, Arteaga E, Aedo S, Arriola-Montenegro J, López M, Martino M, et al. Metformin use is associated with a lower risk of osteoporosis in adult women independent of type 2 diabetes mellitus and obesity. REDLINC IX study, Gynecological endocrinology : the official journal of the International Society of Gynecological Endocrinology 2020;36(5):421–5.
- [34] Zhao J, Li Y, Zhang H, Shi D, Li Q, Meng Y, et al. Preventative effects of metformin on glucocorticoid-induced osteoporosis in rats. *J Bone Miner Metabol* 2019;37(5): 805–14.
- [35] Gao Y, Li Y, Xue J, Jia Y, Hu J. Effect of the anti-diabetic drug metformin on bone mass in ovariectomized rats. *Eur J Pharmacol* 2010;635(1–3):231–6.
- [36] Phimpilhai M, Pothacharoen P, Chattipakorn N, Kongtawelert P. Receptors of advanced glycation end product (RAGE) suppression associated with a preserved osteogenic differentiation in patients with prediabetes. *Front Endocrinol* 2022;13: 799872.
- [37] Liu J, Mao J, Jiang Y, Xia L, Mao L, Wu Y, et al. AGEs induce apoptosis in rat osteoblast cells by activating the caspase-3 signaling pathway under a high-glucose environment in vitro. *Appl Biochem Biotechnol* 2016;178(5):1015–27.
- [38] Huang JS, Lee YH, Chuang LY, Guh JY, Hwang JY. Cinnamaldehyde and nitric oxide attenuate advanced glycation end products-induced the Jak/STAT signaling in human renal tubular cells. *J Cell Biochem* 2015;116(6):1028–38.
- [39] Grimm S, Ott C, Hörlacher M, Weber D, Höhn A, Grune T. Advanced-glycation-end-product-induced formation of immunoproteasomes: involvement of RAGE and Jak2/STAT1. *Biochem J* 2012;448(1):127–39.
- [40] Nowotny K, Jung T, Höhn A, Weber D, Grune T. Advanced glycation end products and oxidative stress in type 2 diabetes mellitus. *Biomolecules* 2015;5(1):194–222.
- [41] Simon AR, Rai U, Fanburg BL, Cochran BH. Activation of the JAK-STAT pathway by reactive oxygen species. *Am J Physiol* 1998;275(6):C1640–52.
- [42] Kim S, Koga T, Isobe M, Kern BE, Yokochi T, Chin YE, et al. Stat1 functions as a cytoplasmic attenuator of Runx2 in the transcriptional program of osteoblast differentiation. *Genes Dev* 2003;17(16):1979–91.
- [43] Tajima K, Takaishi H, Takito J, Tohmonda T, Yoda M, Ota N, et al. Inhibition of STAT1 accelerates bone fracture healing. *J Orthop Res : official publication of the Orthopaedic Research Society* 2010;28(7):937–41.
- [44] Zhang Y, Cao X, Li P, Fan Y, Zhang L, Ma X, et al. microRNA-935-modified bone marrow mesenchymal stem cells-derived exosomes enhance osteoblast proliferation and differentiation in osteoporotic rats. *Life Sci* 2021;272:119204.
- [45] Nahlé S, Pasquin S, Laplante V, Rousseau F, Sharma M, Gauchat JF. Cardiostrophin-like cytokine (CLCF1) modulates mesenchymal stem cell osteoblastic differentiation. *J Biol Chem* 2019;294(32):11952–9.
- [46] Abdelsamia EM, Khaleel SA, Balah A, Abdel Baky NA. Curcumin augments the cardioprotective effect of metformin in an experimental model of type I diabetes mellitus; Impact of Nrf2/HO-1 and JAK/STAT pathways. *Biomed. Pharmacother.* 2019;109:2136–44.
- [47] Marrero MB, Banes-Berclé AK, Stern DM, Eaton DC. Role of the JAK/STAT signaling pathway in diabetic nephropathy. *Am J Physiol Ren Physiol* 2006;290(4): F762–8.
- [48] Ortiz-Muñoz G, Lopez-Parra V, Lopez-Franco O, Fernandez-Vizarrá P, Mallavia B, Flores C, et al. Suppressors of cytokine signaling abrogate diabetic nephropathy. *J Am Soc Nephrol : JASN (J Am Soc Nephrol)* 2010;21(5):763–72.
- [49] Amiri F, Shaw S, Wang X, Tang J, Waller JL, Eaton DC, et al. Angiotensin II activation of the JAK/STAT pathway in mesangial cells is altered by high glucose. *Kidney Int* 2002;61(5):1605–16.
- [50] Wang X, Shaw S, Amiri F, Eaton DC, Marrero MB. Inhibition of the Jak/STAT signaling pathway prevents the high glucose-induced increase in tgf-beta and fibronectin synthesis in mesangial cells. *Diabetes* 2002;51(12):3505–9.
- [51] Kular J, Tickner J, Chim SM, Xu J. An overview of the regulation of bone remodelling at the cellular level. *Clin Biochem* 2012;45(12):863–73.
- [52] Mai QG, Zhang ZM, Xu S, Lu M, Zhou RP, Zhao L, et al. Metformin stimulates osteoprotegerin and reduces RANKL expression in osteoblasts and ovariectomized rats. *J Cell Biochem* 2011;112(10):2902–9.
- [53] Kanazawa I, Yamaguchi T, Yano S, Yamauchi M, Sugimoto T. Metformin enhances the differentiation and mineralization of osteoblastic MC3T3-E1 cells via AMP kinase activation as well as eNOS and BMP-2 expression. *Biochem Biophys Res Commun* 2008;375(3):414–9.
- [54] Zhen D, Chen Y, Tang X. Metformin reverses the deleterious effects of high glucose on osteoblast function. *J Diabetes Complicat* 2010;24(5):334–44.
- [55] Cortizo AM, Sedlinsky C, McCarthy AD, Blanco A, Schurman L. Osteogenic actions of the anti-diabetic drug metformin on osteoblasts in culture. *Eur J Pharmacol* 2006;536(1–2):38–46.
- [56] Yan Z, Tian X, Zhu J, Lu Z, Yu L, Zhang D, et al. Metformin suppresses UHMWPE particle-induced osteolysis in the mouse calvaria by promoting polarization of macrophages to an anti-inflammatory phenotype. *Molecular medicine (Cambridge, Mass.)* 2018;24(1):20.
- [57] Chen Z, Zige L, Sai Kiang Y, Desheng C. Experimental study on the inhibition of RANKL-induced osteoclast differentiation in vitro by metformin hydrochloride. *Int. J. Endocrinol.* 2022;2022:6778332.
- [58] Tao LY, Łagosz-Cwik KB, Hogervorst JMA, Schoenmaker T, Grabiec AM, Forouzanfar T, et al. Diabetes medication metformin inhibits osteoclast formation and activity in in vitro models for periodontitis. *Front Cell Dev Biol* 2021;9:777450.

- [59] Xie X, Hu L, Mi B, Xue H, Hu Y, Panayi AC, et al. Metformin alleviates bone loss in ovariectomized mice through inhibition of autophagy of osteoclast precursors mediated by E2F1, Cell communication and signaling. *CCS* 2022;20(1):165.
- [60] Takeno A, Kanazawa I, Tanaka K, Notsu M, Yokomoto M, Yamaguchi T, et al. Activation of AMP-activated protein kinase protects against homocysteine-induced apoptosis of osteocytic MLO-Y4 cells by regulating the expressions of NADPH oxidase 1 (Nox1) and Nox2. *Bone* 2015;77:135–41.
- [61] Ai Y, Xu R, Liu L. The prevalence and risk factors of sarcopenia in patients with type 2 diabetes mellitus: a systematic review and meta-analysis. *Diabetol Metab Syndrome* 2021;13(1):93.
- [62] Senesi P, Montesano A, Luzzi L, Codella R, Benedini S, Terruzzi I. Metformin treatment prevents sedentariness related damages in mice. *J Diabetes Res* 2016; 2016:8274689.
- [63] Suwa M, Egashira T, Nakano H, Sasaki H, Kumagai S. Metformin increases the PGC-1alpha protein and oxidative enzyme activities possibly via AMPK phosphorylation in skeletal muscle in vivo. *J. Appl. Physiol. (Bethesda, Md 1985;101(6):1685–92.* 2006.
- [64] Sandri M, Lin J, Handschin C, Yang W, Arany ZP, Lecker SH, et al. PGC-1alpha protects skeletal muscle from atrophy by suppressing FoxO3 action and atrophy-specific gene transcription. *Proc Natl Acad Sci USA* 2006;103(44):16260–5.
- [65] Cannavino J, Brocca L, Sandri M, Bottinelli R, Pellegrino MA. PGC1- α over-expression prevents metabolic alterations and soleus muscle atrophy in hindlimb unloaded mice. *J Physiol* 2014;592(20):4575–89.